Sensors and Materials, Vol. 22, No. 3 (2010) 109–120
MYU Tokyo

S & M 0793

Micropatterning of Poly (*N*-isopropylacrylamide) (PNIPAAm) Hydrogels: Effects on Thermosensitivity and Cell Release Behavior

Huijie Hou, Yaping Hou[1], Melissa A. Grunlan[1], Dany J. Munoz-Pinto[2], Mariah S. Hahn[2] and Arum Han[*]

Department of Electrical and Computer Engineering Texas A&M University, College Station, TX 77843-3128, USA
[1]Department of Biomedical Engineering Texas A&M University, College Station, TX 77843-3128, USA
[2]Department of Chemical Engineering Texas A&M University, College Station, TX 77843-3128, USA

(Received February 5, 2009; accepted September 9, 2009)

Key words: thermoresponsive hydrogel, PNIPAAm, photopolymerization, cell release, micropatterning

The thermally driven, reversible change in the surface properties of poly (*N*-isopropylacrylamide) (PNIPAAm) hydrogels from a hydrophilic (water-swollen) state to a hydrophobic (deswollen) state when heated above the volume phase transition temperature (VPTT, ~35°C) makes them useful in inducing controlled cell release. To improve the kinetics of swelling and deswelling, we have prepared microstructured (i.e., micropillared) thermoresponsive surfaces comprising pure PNIPAAm hydrogel and nanocomposite PNIPAAm hydrogel embedded with polysiloxane colloidal nanoparticles (~220 nm diameter, 1 wt%) via photopolymerization. The thermosensitivity (i.e., degree and rate of swelling/deswelling) of these surfaces and how it can be regulated using different micropillar sizes and densities were characterized by measuring the dynamic size changes in micropillar dimensions in response to thermal activation. Our results show that the dynamic thermal response rate can be increased by more than twofold when the micropillar size is reduced from 200 to 100 μm. The temperature-controlled cell release behaviors of pure PNIPAAm and nanocomposite PNIPAAm micropatterned surfaces were successfully characterized using mesenchymal progenitor cells (10T½). This study demonstrates that the thermosensitivity of PNIPAAm surfaces can be regulated by introducing micropillars of different sizes and densities, while maintaining good temperature-controlled cell release behavior.

[*]Corresponding author: e-mail: arum.han@ece.tamu.edu

1. Introduction

Materials that can respond to external stimulus are of great interest as smart materials for various biomedical applications.[1,2] Thermoresponsive hydrogels reversibly switch from a water-swollen to a deswollen state in response to temperature changes. The most widely studied are poly(*N*-isopropylacrylamide) (PNIPAAm) hydrogels, which have a volume phase transition temperature (VPTT) of ~ 35°C.[3] Thus, they are hydrated (swollen) below VPTT and become dehydrated (deswollen) when heated above VPTT. In addition, the surfaces of PNIPAAm hydrogels undergo a discontinuous change from a hydrophilic state to a hydrophobic state when heated above VPTT.[4] Reversible, temperature-induced changes in the volume and surface properties of PNIPAAm hydrogels have prompted their use in various biomedical applications such as in drug delivery.[5] In addition, PNIPAAm hydrogels have been used for bioseparation[6] as they can be separated from water at temperatures above VPTT and for protein refolding applications[7] owing to their high effectiveness in enhancing protein renaturation.

Thermoresponsive polymers such as PNIPAAm have been studied for their temperature-dependent foul-releasing or self-cleaning behavior.[8–12] In aqueous solution, linear PNIPAAm becomes insoluble upon heating above its lower critical solution temperature (LCST) of ~35°C, which can then be reversed upon cooling.[13] Crosslinked PNIPAAm hydrogels reversibly change from a water-swollen state to a shrunken (deswollen) state by exuding water when heated above their VPTT of ~35°C.[14–17] As a result, both covalently grafted PNIPAAm chains and PNIPAAm hydrogels display a pronounced increase in surface hydrophobicity when heated above their LCST or VPTT, respectively.[9] Thus, the thermal modulation of both PNIPAAm-grafted surfaces and PNIPAAm hydrogels has been used to induce the release of cells.[9–12,18–20] For instance, the "cell releasing" property of PNIPAAm hydrogels has been exploited for their use as substrates for cell culture[21] and tissue engineering, in which the cells adhere to the surface during a particular stage of the experiment but can be released as a cell sheet at a later time point by thermal activation.[22]

The extent of cell release can be controlled by regulating the degree and rate of PNIPAAm hydrogel swelling/deswelling (i.e., their thermosensitivity). Compositional and physical alterations to PNIPAAm hydrogels, including the formation of interpenetrating polymer networks, have been explored to improve thermal response kinetics.[23,24] An alternative approach to improve the thermosensitivity of PNIPAAm hydrogels is to reduce their millimeter dimensions to micron scale. The reduction in gel size takes advantage of the fact that the kinetics of swelling and deswelling are proportional to the square of the smallest dimension.[25,26] PNIPAAm hydrogels have been fabricated as micron-scale pillars and other such structures that exhibit faster response times.[26,27]

The thermosensitivity of planar, millimeter thick PNIPAAm hydrogels[3,4,35] and microporous hydrogels[28,29] as well as PNIPAAm-based colloidal particles[30,31] has been studied. However, the degree to which microscale surface topography, such as the size and density of a micropillar surface array, affects PNIPAAm thermosensitivity has not been well studied. Furthermore, there are limited reports on the release of cells

from microscale PNIPAAm hydrogel structures[32–36] and no studies, to the best of our knowledge, relating the effect of pillar dimensions and patterns to cell release behavior.

In this study, we examined the thermosensitivity of micoscale PNIPAAm pillars, both with polysiloxane colloidal nanoparticles incorporated within hydrogel structures and without the nanoparticles. Previously, we have shown that the incorporation of colloidal polysiloxane nanoparticles could alter the swelling behavior and surface properties of planar PNIPAAm hydrogels while maintaining the VPTT of pure PNIPAAm hydrogels, and at the same time be mechanically stronger.[2] Pure and nanocomposite PNIPAAm hydrogel micropatterned surfaces were fabricated having micropillar arrays 100–200 μm in diameter and 100 μm in height with various separations using a simple photopolymerization method. The effects of micropillar size and separation on the static and dynamic thermal responses of such surfaces were determined here via changes in pillar dimensions using optical microscopy. Finally, the release of mesenchymal progenitor cells (10T½) cultured on swollen microstructured PNIPAAm and nanocomposite surfaces at 30°C (below VPTT) was evaluated. Thus, the micropatterning of PNIPAAm hydrogels may improve their performance in applications such as cell release, cell coculture, and microfluidic applications.[37–39]

2. Materials and Methods

2.1 *Materials*

Octamethylcyclotetrasiloxane (D_4) and 1,3,5,7-tetramethyl-1,3,5,7-tetravinyl-cyclotetrasiloxane (D_4^{Vi}) were purchased from Gelest Inc. (Morrisville, PA). Dodecylbenzensulfonic acid (DBSA, BIO-SOFT® S-101) was purchased from Stepan Co. (Northfield, IL). Potassium persulfate ($K_2S_2O_8$), *N*-isopropylacrylamide (NIPAAm, 97%), 2,2-dimethyl-2-phenyl-acetophenone (DMAP), and solvents were purchased from Aldrich (St. Louis, MO). *N*,*N*'-methylenebisacrylamide (BIS, 99%) was obtained from Acros Organics (Morris Plane, NJ). 1-[4-(2-Hydroxy-ethoxy)-phenyl]-2-hydroxy-2-methyl-1-propane-1-one (Irgacure® 2959) was obtained from Ciba Chemical (Tarrytown, NY). Dulbecco's modified eagle medium (DMEM) and penicillin/streptomycin/amphotericin were obtained from Mediatech (Herndon, VA). Fetal bovine serum (FBS) was obtained from Hyclone (Logan, UT). All reagents were used as received.

2.2 *Preparation of hydrogel aqueous precursor solutions*

Crosslinked polysiloxane colloidal nanoparticles were prepared by the cationic emulsion polymerization of D_4 and D_4^{Vi} as previously described.[2] The nanoparticles were purified via dialysis (Slide-A-Lyzer® Dialysis Cassette, MWCO = 10,000, Pierce Chemical Co., Rockford, IL.) against daily changes of deionized (DI) water for 3 days. The emulsion solid content was 8.5%. Dynamic light scattering (DLS) showed an average diameter of 219 nm and polydispersity (PD) of 0.10 with particle sizes ranging from 106 to 531 nm.

Aqueous precursor solutions (12.5 wt%) containing NIPAAm monomer, BIS crosslinker, Irgacure-2959 photoinitiator, and optionally, for the nanocomposite hydrogel, 1.0% polysiloxane nanoparticles (wt% solids of nanoparticles with respect

to total precursor solution weight) were prepared as follows. In a 50 mL round bottom flask equipped with a Teflon™-coated stir bar, NIPAAm (1.0 g, 8.84 mmol), BIS (0.02 g, 0.13 mmol), and Irgacure-2959 (0.08 g, 0.36 mmol) were dissolved in DI water (the total volume is 7 mL including the volume of water introduced later by the nanoparticle emulsion), and the solution was stirred under N_2 for 15 min. Finally, an appropriate amount of emulsion containing polysiloxane nanoparticles was added, and the mixture was stirred for 10 min under N_2.

2.3 *Photopolymerization of precursor solutions to form micropillar arrays*

Glass slides onto which hydrogel micropillars are formed were cleaned by soaking in piranha solution (H_2O_2:H_2SO_4 = 1:3 v/v) for 30 min, followed by thoroughly washing with DI water and blow drying with N_2. Glass slides serving as covers were cleaned with acetone and isopropanol followed by thoroughly washing with DI water. Aqueous precursor solutions for pure PNIPAAm hydrogel and nanocomposite hydrogel (containing 1 wt% polysiloxane nanoparticles) were each used to fill the gap between the two cleaned glass slides (top: "Piranha" cleaned glass, bottom: solvent cleaned glass) that were separated by a 100-μm-thick spacer that defined the height of the micropillars. A photolithography mask with circular patterns with diameters of 100 and 200 μm was placed on top of the piranha-cleaned glass side of the sandwiched structure. Since PNIPAAm hydrogels formed below 20°C are morphologically homogeneous and mechanically stronger,[40–42] this structure was immersed in an ice water bath (~7°C) for 2 min, and then exposed to UV light (Omnicure Series 1000, 15 mW/cm^2, 365 nm, Plano, TX) for 40 s to induce polymerization. Figure 1 shows the overall fabrication setup. After photopolymerization, the mask and cover glass slide were removed, and impurities were removed by carefully washing with DI water. The sample was then placed under a fume hood for 3 days to dry before testing. Micropillars with diameters of 200 μm (with 100 and 300 μm spacings) and 100 μm (with 50 and 150 μm spacings) were fabricated with both pure PNIPAAm and nanocomposite hydrogels. Analogous hydrogel sheets were also prepared (100 μm thick) using the same method but without the mask.

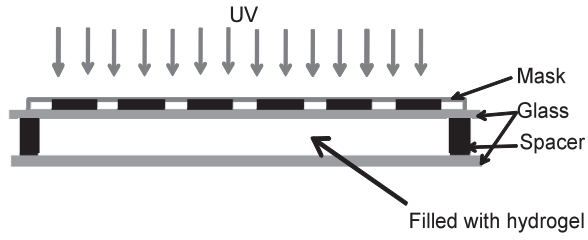

Fig. 1. Illustration of the hydrogel micropillar fabrication setup using photopolymerization combined with a photolithography mask. The thickness of the spacer determines the height of the micropillar.

2.4 *Temperature-modulated dynamic swelling-deswelling characterization*

The dynamic thermal response of hydrogel micropillars was examined by measuring the time-dependent diameter change during thermal cycling. Specimen temperature was controlled by taping a glass slide with hydrogel micropatterns onto the top of a thermal heater with a thermal ribbon sensor (Minco Inc., Midway, TN) and controlled by a thermostat (CT16A2, Minco Inc.). DI water was dispensed on top of the samples using a pipette to cover the micropillar arrays with water. After 15 min or when the size of the micropillars became constant, temperature was continuously cycled between ~26°C (below VPTT) and 45°C (above VPTT) at a heating rate of 1.02°C/s (measured rate from 30 to 40°C) and a cooling rate of 0.03°C/s (measured rate from 40 to 30°C) to observe the deswelling and swelling behaviors of hydrogel micropillars. Both time and temperature were recorded, and images were continuously acquired using a microscope (ECLIPSE LV100D, Nikon Inc. Melville, NY) equipped with a CCD camera. The top diameters of the hydrogel micropillars were measured from these microscope images. Using this method, the dynamic thermal response of groups of micropillars with average diameters of 200 and 100 μm for both PNIPAAm and nanocomposite PNIPAAm were respectively characterized.

2.5 *Imaging of hydrogel micropillar arrays*

Scanning electron microscopy (SEM) was used to determine the pillar diameter of hydrogel micropillar arrays. Air-dried micropillar arrays were subjected to Au/Pt sputter coating and viewed by SEM (JEOL JSM 6400) at an acceleration voltage of 15 keV.

2.6 *Cell preparation*

Cryopreserved 10T½ mesenchymal progenitor cells obtained from the American Type Culture Collection (ATCC, Manassas, VA) were thawed and expanded in monolayer culture in accordance with ATCC protocols. Until the time of harvest, the cells were maintained at 37°C/5% CO_2 in DMEM supplemented with 10% heat-inactivated FBS, 10 U/mL penicillin, 10 g/L streptomycin, and 10 g/L amphotericin (1% PSA).

2.7 *Temperature-dependent cell release behavior*

Two-hundred micrometer diameter pillar arrays with a 100 μm spacing (i.e., 200_1R) were prepared from both pure PNIPAAm and nanocomposite hydrogels on glass as mentioned above, followed by soaking for two days in PBS and by sterilization via irradiation with UV light for 1 h. The surfaces of the pillar arrays were coated with DMEM supplemented with 40% FBS and antibiotics (PSA) for 1 h at 30° (below VPTT) to force PNIPAAm-based hydrogel pillars into a water-swollen, hydrophilic state and to equilibrate the hydrogels with the cell culture medium. The medium was then drained, and 10T½ cells in a fresh medium containing 10% serum were seeded onto each hydrogel surface (~270,000 cells/cm^2).

After incubation at 30°C for 1.5 h, the arrays were transferred to a Zeiss Axiovert A200 microscope (Carl Zeiss, Germany) equipped with a plate incubation chamber with a temperature controller (Carl Zeiss, Germany) preheated to 30°C. The temperature of the incubation plate was then set to 37°C (above VPTT), and heating progressed at a

rate of ~ 2°C/min, thereby causing the pillars to deswell and become hydrophobic. The arrays were held at 37°C for 5 min and then allowed to air-cool (~ 2°C/min) to 30°C. This heating and cooling cycles were repeated until the onset of cell sheet delamination. For each cycle, images were captured in the initial swollen and final deswollen states.

2.8 *Statistical analysis*

To see statistical significance when comparing results, a two-sample pooled T-test at a significance level of 1% was performed.

3. Results and Discussion

3.1 *Microfabrication of hydrogel micropillar array*

The photopolymerization of hydrogel is a rapid and facile means of fabricating microstructures where patterns on a photolithography mask define shape of the microstructures. A spacer that creates a gap between two glass slides into which liquid precursor is poured defines the height of microstructures. Figure 2 shows images of micropillars prepared from pure PNIPAAm and nanocomposite hydrogels using a mask with 200- and 100-μm-diameter circular patterns. Because the samples were dried for SEM, these micropillars exhibit diameters smaller than their original pattern size on the mask. For micropillars made of nanocomposite hydrogel, polysiloxane nanoparticles embedded in the micropillar structure can be clearly seen (Figs. 2(c) and 2(d)).

3.2 *Thermosensitivity of hydrogel micropillars*

Microstructured hydrogels of smaller dimensions are predicted to swell and deswell more significantly and faster owing to the shorter equilibrium time required and the availability of space for swelling. The effects of micropillar dimensions on the extent and rate of swelling and deswelling of microstructured pure PNIPAAm and nanocomposite

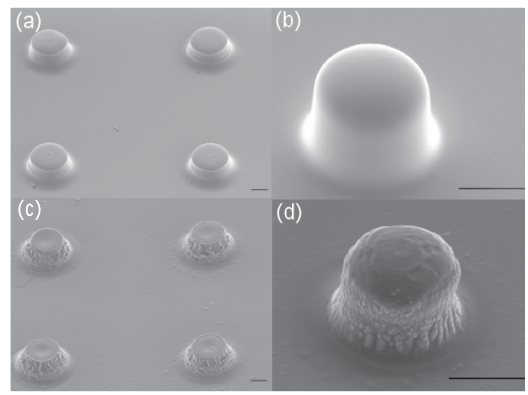

Fig. 2. SEM images of micropillars: (a) and (b) pure PNIPAAm micropillars; (c) and (d) nanocomposite PNIPAAm (containing 1.0 wt% polysiloxane nanoparticles). Sizes: (a) and (c) 200 μm diameter; (b) and (d) 100 μm diameter. All scale bars are 50 μm.

hydrogels were compared. Micropillars with average diameters of 120 and 210 μm were compared. Optical images were captured before and after the thermal equilibration of hydrated hydrogel micropillars from 25°C (below VPTT) to 45°C (above VPTT) (Fig. 3). The extent of micropillar shrinking is reflected by the maximum shrinking ratio defined as D_{min}/D_{max}, where D_{min} is the minimum micropillar diameter in its deswollen state at 45°C, and D_{max} is the maximum micropillar diameter at 25°C. The diameters of the top part of the micropillars were used for measurements.

The maximum shrinking ratios of 210 and 120 μm micropillars were 73 and 35%, respectively, for pure PNIPAAm micropillars, and were 62 and 44%, respectively, for the nanocomposite micropillars (Table 1). Thus, smaller (120 μm diameter) micropillars shrank more significantly than larger (210 μm diameter) micropillars of the same composition. Furthermore, reducing the micropillar size produced greater deswelling for pure PNIPAAm micropillars than for nanocomposite hydrogel micropillars, likely owing to the presence of hydrophobic polysiloxane nanoparticles.

The three-dimensional shape of the PNIPAAm micropillars after shrinking could not be directly measured, but could be predicted indirectly through optical microscopy. As can be seen in the differential interference contrast (DIC) images in Fig. 3, the cylinder-shaped micropillar structures changed into cone-shaped pillar structures once deswollen. This phenomenon can be easily seen in Figs. 3(b) and 3(d) where the contrast difference is easily observable. The overall size, including the bottom part of the micropillar, decreased as well, implying that parts of the bottom PNIPAAm micropillars were not attached firmly to the substrate anymore after one thermocycle. Once swollen again, the shape returns to its original cylinder shape.

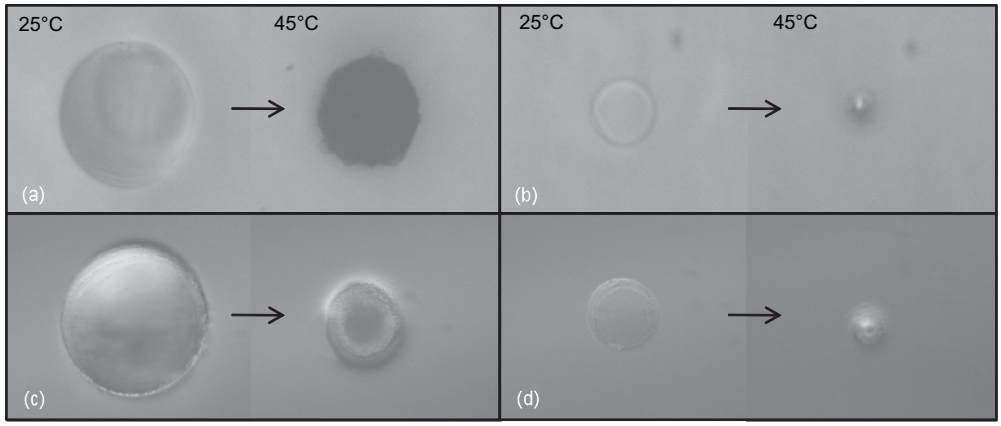

Fig. 3. Microscopy images showing thermal activation of micropillars when temperature was increased above VPTT. (a) Pure PNIPAAm micropillar with original size of 210 μm shrinking to 159 μm. (b) Pure PNIPAAm micropillar with original size of 100 μm shrinking to 30 μm. (c) Nanocomposite PNIPAAm (1.0 wt% polysiloxane nanoparticle) micropillar with original size of 226 μm shrinking to 128 μm. (d) Nanocomposite PNIPAAm (1.0 wt% polysiloxane nanoparticle) micropillar with original size of 110 μm shrinking to 50 μm.

Table 1
Thermal responses of micropillars with different diameters and compositions.

Sample	Diameter (μm)	D_{min}/D_{max}	Swelling ratio	Deswelling ratio
Pure PNIPAAm	210	0.73	0.10	0.54
	120	0.35	0.33	1.81
Nanocomposite PNIPAAm	210	0.62	0.16	0.55
	120	0.44	0.52	1.15

The rate of deswelling of these micropillars was also determined during thermal cycling from a temperature below VPTT to that above VPTT and back to below VPTT (Table 1, Fig. 4). To analyze the shrinking (deswelling) rate of micropillars, the rate of temperature increase was set sufficiently high (0.3°C/s) so that micropillar shrinking rate was not limited by the rate of temperature change. Normalized diameter (D/D_0) was used to compare the swelling and deswelling rates of micropillars with different sizes and different compositions, where D is the dynamic diameter of micropillars during heating and D_0 is the original diameter of micropillars in the swollen state at 25°C (below VPTT). Again, the diameters of the top of the micropillars were used. In Fig. 4(a), pure PNIPAAm micropillars with average initial diameters of 210 and 120 μm were compared. During heating to 40°C (i.e., the first 40 s), the shrinking rate of the 120- and 210-μm-diameter micropillars were 1.81±0.10 and 0.54±0.04%/s (average ± standard deviation from three samples), respectively. Thus, the 120 μm micropillars deswelled 3.3-fold faster. During subsequent cooling from 40°C to RT (i.e., from 510 to 645 s), the swelling rates of the 120 and 210 μm micropillars were 0.33±0.03 and 0.10±0.01%/s, respectively. Thus, the 120 μm micropillars swelled 3.4-fold faster.

The shrinking rates of micropillars of the nanocomposite hydrogels with average diameters of 120 and 210 μm were 1.15±0.10 and 0.55±0.08%/s, respectively. Thus, the 120-μm-diameter micropillar shrank 2.1-fold faster (Fig. 4(b)). The subsequent swelling rates of these two micropillars were 0.52±0.06 and 0.16±0.04%/s, respectively. Thus, the 120-μm-diameter micropillars swelled 3.2-fold faster.

These above-mentioned results clearly demonstrate that the dynamic thermal response of hydrogel micropillars is size-dependent, where smaller micropillars have significantly faster swelling and deswelling dynamics. By decreasing micropillar size from about 200 to 100 μm, thermal response rate increases by at least twofold. When comparing the thermal activation of pure PNIPAAm micropillars to that of nanocomposite micropillars, no significant difference could be observed for the 210-μm-diameter micropillars. However, when the micropillar diameter was decreased to 120 μm, both the shrinking and swelling rates of pure PNIPAAm micropillars became significantly higher than those of nanocomposite micropillars. These experiments demonstrate that, when using surfaces made of microstructured hydrogels, thermosensitivity may be controlled by adjusting hydrogel microstructure size.

3.3 *Temperature-dependent cell release behavior*

Cell release behavior that demonstrates the self-cleaning ability of micropatterned hydrogels was examined with 200-μm-diameter micropillar arrays with a 100 μm

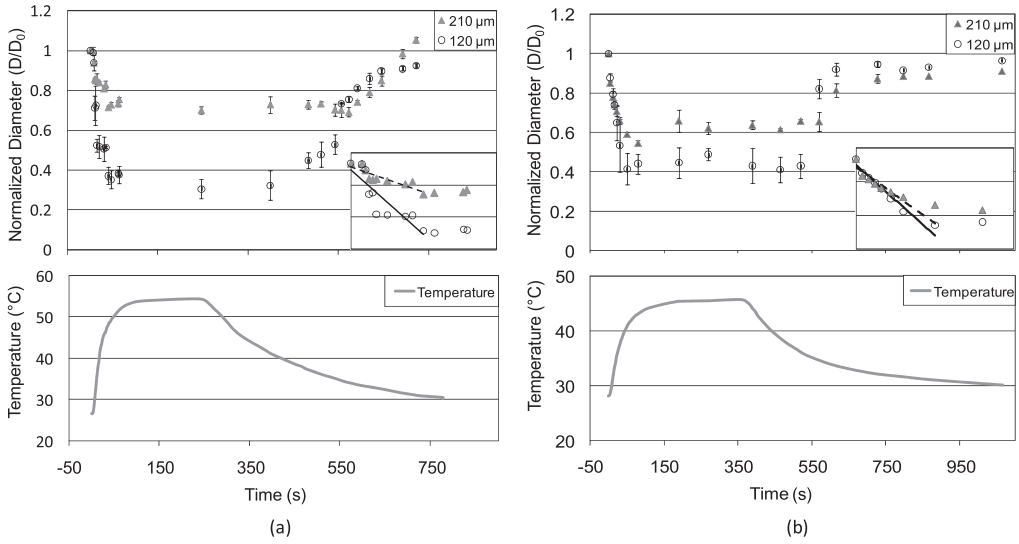

Fig. 4. Dynamic thermal responses of 210- and 120-μm-diameter micropillars made of (a) pure PNIPAAm and (b) nanocomposite PNIPAAm (1.0 wt% polysiloxane nanoparticle). (Standard deviations were from three samples with similar diameters and are marked on the graph.)

separation (200_1R). Both pure PNIPAAm and nanocomposite PNIPAAm were used to fabricate microstructured surfaces. Figure 5(a) shows the cell release characteristics of microstructured surfaces made of pure PNIPAAm. It can be seen that the entire cell sheet began to detach and fold from the hydrogel surface at the end of the second heating/cooling cycle. This is due to the fact that these cells form a connected cell layer, and once multiple points of the cell layer start coming off due to PNIPAAm micropillar actuation, the entire sheet quickly detaches. The fact that cell sheets can detach easily through thermocycling even with a low-density (*e.g.*, loosely packed) micropillar array shows the feasibility of a self-cleaning surface to mitigate cell attachment. For the nanocomposite PNIPAAm microstructured surface (Fig. 5(b)), five thermal cycles (heating and cooling) were applied to initiate cell sheet detachment from the surface. More thermal cycles were needed for nanocomposite PNIPAAm microstructured surfaces to release the cell sheet. This is probably due to the stronger initial cell attachment onto nanocomposite hydrogels, which is induced by the more hydrophobic surface property of nanocomposite hydrogels. However, these preliminary studies show that nanocomposite hydrogel microstructured surfaces still exhibit a self-cleaning ability. We expect that nanocomposite PNIPAAm hydrogels, with their better mechanical properties and potential for self-cleaning, will be of benefit in coating insertion biosensors and other devices. Our ability to modulate the rate of swelling and deswelling of both nanocomposite and pure NIPAAm hydrogels by introducing microstructural complexity while retaining VPTT and the cell release behavior of planar NIPAAm hydrogels will serve as an additional tool to exploit in surface coating applications.

(a)

(b)

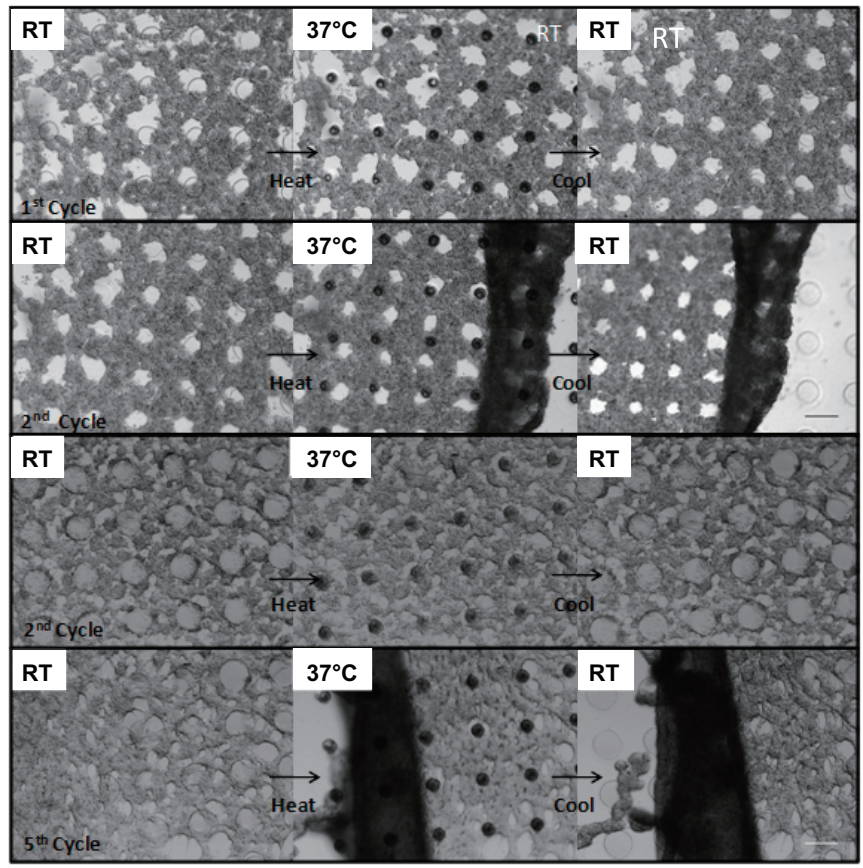

Fig. 5. Time-lapsed images of mesenchymal progenitor cells (10T½) on hydrogel pillar arrays at initial swollen stage (at RT, below VPTT) and during thermal cycling (heat to 37°C, above VPTT). The cell sheet began to detach and fold as the pillars were forced through cyclical deswelling and swelling stages. (a) Pure PNIPAAm and (b) nanocomposite PNIPAAm microstructured surfaces (Scale bars: 200 μm).

4. Conclusions

In this study, we microfabricated thermoresponsive hydrogel surfaces that exhibit self-cleaning behavior with arrays of micropillars with different sizes and densities made of both pure PNIPAAm and nanocomposite PNIPAAm using photopolymerization. The static and dynamic thermoresponsivenesses of these surfaces at temperatures below and above VPTT were determined. Our results show that thermoresponsiveness characterized by the swelling and deswelling rates and ratio can be markedly increased by reducing micropillar size. The cell release experiments on these microstructured

pure PNIPAAm and nanocomposite PNIPAAm surfaces demonstrate good cell release behavior through thermal cycling. Our results demonstrate that microstructured PNIPAAm and nanocomposite hydrogel surfaces have enhanced thermosensitivity and surface property changes compared with analogous planar surfaces. Compared with traditional methods of modifying PNIPAAm thermoresponsiveness, the use of microstructured surfaces can markedly increase response time when thermally activated, resulting in surfaces that can rapidly and effectively respond to changes in temperature, as well as increase the efficiency of self-cleaning ability.

Acknowledgements

The authors thank Mr. Jaewon Park for taking the SEM images of the hydrogel micropillars and Ms. Ranjini Murthy for helpful experimental procedure discussions. This project was funded by the Korean Ministry of Knowledge Economy and Seoul Technopark under grant #1002970790 and the National Science Foundation (NSF) under grant #0854462.

References

1 I. Hirata, M. Okazaki and H. Iwata: Polymer **45** (2004) 5569.
2 Y. Hou, A. M. Smitherman, A. S. Bulick, M. S. Hahn, H. Hou *et al.*: Biomaterials **29** (2008) 3175.
3 J. Zhang, R. Pelton and Y. Deng: Langmuir **11** (1995) 2301.
4 T. Yakushiji, K. Sakai, A. Kikuchi, T. Aoyagi, Y. Sakurai *et al.*: Anal. Chem. **71** (1999) 1125.
5 Y. Qiu and K. Park: Adv. Drug Delivery Rev. **53** (2001) 321.
6 Z. M. O. Rzaev, S. Dincer and E. Piskin: Prog. Polym. Sci. **32** (2007) 534.
7 A. S. Ashok Kumar, I. Y. Galaev and B. Mattiasson: Prog. Polym. Sci. **32** (2007) 1205.
8 M. E. Callow, J. A. Callow, L. K. Ista, S. E. Coleman, A. C. Nolasco *et al.*: Appl. Environ. Microbiol. **66** (2000) 3249.
9 L. K. Ista, V. H. Perez-Luna and G. P. Lopez: Appl. Environ. Microbiol. **65** (1999) 1603.
10 L. K. Ista and G. P. Lopez: J. Indust. Microbiol. Biotech. **20** (1998) 121.
11 D. Cunliffe, C. d. l. H. Alarcón, V. Peters, J. R. Smith and C. Alexander: Langmuir **19** (2003) 2888.
12 D. Cunliffe, C. A. Smart, J. Tsibouklis, S. Young, C. Alexander *et al.*: Biotech. Lett. **22** (2000) 141.
13 O. Chiantore, M. Guaita and L. Trossarelli: Makromol. Chem. **180** (1979) 969.
14 T. Tanaka, E. Sato, Y. Hirokawa, H. Hirotsu and I. Peezermans: Phys. Rev. Lett. **55** (1990) 2455.
15 L. D. Taylor and L. D. Cerankowski: J. Polym. Sci., Part A: Polym. Chem. **13** (1975) 2551.
16 Y. Hirokawa and T. Tanaka: J. Chem. Phys. **81** (1984) 6379.
17 Y. H. Bae, T. Okano and S. W. Kim: J. Polym. Sci. Part B: Polym. Phys. **28** (1990) 923.
18 A. S. Hoffman: Adv. Drug Delivery Rev. **54** (2002) 3.
19 D. Schmaljohann: e-Polymers **021** (2005) 1.
20 T. Okano, N. Yamada, H. Sakai and Y. Sakurai: J. Biomed. Mater. Res., B **27** (1993) 1243.
21 T. Aoki, Y. Nagao, E. Terada, K. Sanui, N. Ogata *et al.*: J. Biomater. Sci., Polym. Ed. **7** (1995) 539.
22 M. Yamato, M. Utsumi, A. Kushida, C. Konno, A. Kikuchi *et al.*: Tissue Eng. **7** (2001) 473.

23 S. Zhou and C. Wu: Macromolecules **29** (1996) 4998.
24 S. H. Gerke: Adv. Polym. Sci. **110** (1993) 81.
25 D. Chandra, J. A. Taylor and S. Yang: Soft Matter. **4** (2008) 979.
26 D. Kuckling, J. Hoffman, M. Plotner, D. Ferse, K. Kretschmer *et al.*: Polymer **44** (2003) 4455.
27 G. Chen, Y. Imanishi and Y. Ito: J. Biomed. Mater. Res. **42** (1998) 38.
28 Z. X. Zhao, Z. Li, Q. B. Xia, E. Bajalis and H. X. Xi: Chem. Eng. J. **142** (2008) 263.
29 X. Zhang, G. Sun, D. Wu and C. Chu: J. Mat. Sci.: Mater. Med. **15** (2004) 865.
30 C. Chen and M. Akashi: Langmuir **13** (1997) 6465.
31 T. Mori and M. Maeda: Langmuir **20** (2004) 313.
32 P. Judeinstein and C. Sanchez: J. Mater. Chem. **6** (1996) 511.
33 T. Meyer, T. Hellweg, S. Spange, S. Hesse, C. Jager *et al.*: J. Polym. Sci. Part A: Polym. Chem. **40** (2002) 3144.
34 O. Fichet, F. Vidal, J. Laskar and D. Teyssie: Polymer **46** (2005) 37.
35 J. H. Park and Y. H. Bae: Biomaterials **23** (2002) 1797.
36 D. A. Stone and H. R. Allcock: Macromolecules **39** (2006) 4935.
37 Y. Tsuda, A. Kikuchi, M. Yamato, A. Nakao, Y. Sakurai *et al.*: Biomaterials **26** (2005) 1885.
38 D. J. Beebe, J. S. Moore, J. M. Bauer, Q. Yu, R. H. Liu *et al.*: Nature **404** (2000) 588.
39 M. E. Harmon, M. Tang and C. W. Frank: Polymer **44** (2003) 4547.
40 C. Sayil and O. Okay: Polym. Bull. **45** (2000) 175.
41 S. Ju, L. Chu, Z. Zhu, L. Hu, H. Song *et al.*: Smart Mater. Struct. **15** (2006) 1767.
42 N. Kayaman, D. Kazan, A. Erarslan, O. Okay and B. M. Baysal: J. Appl. Polym. Sci. **67** (1998) 805.